Published in final edited form as:
Dev Biol. 2014 January 1; 385(1): 41–51. doi:10.1016/j.ydbio.2013.10.016.

Dkk1 in the Peri-Cloaca Mesenchyme Regulates Formation of Anorectal and Genitourinary Tracts

Chaoshe Guo[#a], **Ye Sun**[#a], **Chunming Guo**[#a], **Bryan T. MacDonald**[b], **Joseph G. Borer**[a], and **Xue Li**[a]

[a]Department of Urology, Department of Surgery and Pathology; Boston Children's Hospital, 300 Longwood Avenue; Harvard Medical School, Boston, Massachusetts 02115, USA

[b]The F. M. Kirby Neurobiology Center, Department of Neurology; Boston Children's Hospital, 300 Longwood Avenue; Harvard Medical School, Boston, Massachusetts 02115, USA

[#] These authors contributed equally to this work.

Abstract

Anorectal malformation (ARM) is a common birth defect but the developmental history and the underlying molecular mechanism are poorly understood. Using murine genetic models, we report here that a signaling molecule Dickkopf-1 (*Dkk1*) is a critical regulator. The anorectal and genitourinary tracts are major derivatives of caudal hindgut, or the cloaca. *Dkk1* is highly expressed in the dorsal peri-cloacal mesenchymal (dPCM) progenitors. We show that deletion of *Dkk1* causes the imperforate anus with rectourinary fistula. Mutant genital tubercles exhibit a preputial hypospadias phenotype and premature urethral canalization. *Dkk1* mutants have an ectopic expansion of the dPCM tissue, which correlates with an aberrant increase of cell proliferation and survival. This ectopic tissue is detectable before the earliest sign of the anus formation, suggesting that it is most likely the primary or early cause of the defect. Deletion of *Dkk1* results in an elevation of the *Wnt/ß-catenin* activity. Signaling molecules *Shh*, *Fgf8* and *Bmp4* are also upregulated. Furthermore, genetic hyperactivation of *Wnt/ß-catenin* signal pathway in the cloacal mesenchyme partially recapitulates *Dkk1* mutant phenotypes. Together, these findings underscore the importance of *DKK1* in regulating behavior of dPCM progenitors, and suggest that formation of anus and urethral depends on *Dkk1*-mediated dynamic inhibition of the canonical *Wnt/ß-catenin* signal pathway.

INTRODUCTION

The embryonic hindgut, or the cloaca, is the primordial organ of the anorectal structure as well as the genitourinary tract. Inborn errors resulting in the anorectal malformation (ARM) affect approximately 1/2,500 of live births (Cuschieri, 2002). The process of normal anorectal development, however, remains poorly understood and a major subject of ongoing debate (Hynes and Fraher, 2004; Kluth, 2010).

Address correspondence to: Xue (Sean) Li, Room 1061.4, Enders Research Building, Boston Children's Hospital, Harvard Medical School, 300 Longwood Ave, Boston, MA, 02115, USA. Phone: (617) 919-2703; Fax: (617) 730-0530; sean.li@childrens.harvard.edu..

Historically, the morphogenetic process that separates the anorectal structure from the genitourinary tract has been described as the cloacal septation (Rathke, 1832; Retterer, 1890; Tourneux, 1888). Theories underlying this prevailing view are that local expansion of the cloacal mesenchyme from the rostral end (Tourneux, 1888), bilateral sides (Rathke, 1832; Retterer, 1890) or both (Stephens et al., 2002) leads to formation of the putative urorectal septum (URS). The general thought is that the putative URS, consisting the intra-cloacal mesenchyme (ICM), divides the cloaca into the dorsal anorectal tract and the ventral genitourinary tract (Figure 1A-C). However, careful examinations of developmental history of the normal cloaca morphogenesis (Paidas et al., 1999; Penington and Hutson, 2003) and animal models with the ARM defect have led to a rejection of the septation theory (Kluth et al., 1995; Liu et al., 2003; Nakata et al., 2009; Suda et al., 2011; van der Putte, 1986). Instead, these studies suggest that morphogenesis of the cloaca depends primarily on formation and shift of the cloacal membrane (CM) (Kluth et al., 1995; van der Putte, 1986).

While signal(s) from cloaca endoderm actively participate growth and patterning of surrounding mesenchyme (Lin et al., 2009; Miyagawa et al., 2009a; Seifert et al., 2009; Seifert et al., 2010), we believe that asymmetric growth of surrounding cloacal mesenchyme is the driving force in reshaping the cloaca and separating the anorectal and the genitourinary tract. Our previous genetic fate mapping and mouse mutant studies suggest that the process of transforming the cloaca is reminiscent to the vascular occlusion (Figure 1a'-c') (Wang et al., 2011; Wang et al., 2013). This model is supported by the fact that some remnant of the cloaca, the cloacal duct (CD), can be found at the midline epithelial perineal surface (Seifert et al., 2008).

While these models are not mutually exclusive, each model has distinct features and implications. A key feature of the proposed occlusion model is the asymmetric growth of the cloacal mesenchyme along rostrocaudal and dorsoventral axes (Wang et al., 2011; Wang et al., 2013). Along these two axes, the CM and the dorsal peri-cloacal mesenchymal (dPCM) are two critical pivot points (Figure 1). The dPCM refers to a cell population that locates at the caudal extreme of the cloaca between tail and developing genital tubercle. Specifically, the CM is devoid of mesenchymal cells, and the dPCM progenitors and the adjacent hindgut have a high rate of cell death and low rate of proliferation (Wang et al., 2013). Because of these two pivot points, asymmetric growth along the rostrocaudal axis results in the occlusion of the cloacal cavity, therefore, division of the cloaca (Figure 1a'-c'). At the same time, asymmetric growth along dorsoventral axis leads to the genital tubercle outgrowth (Wang et al., 2013). This outgrowth results in a displacement of the cloacal membrane from a parallel to a perpendicular orientation to the body plan. Because of this displacement, a reversal of dorsoventral axis is adopted in the standard nomenclature to describe cloaca and genital tubercle, i.e. ventral of the cloaca becomes dorsal of the genital tubercle (compare Figure 1A and C). The cloacal occlusion model suggests that the future anal orifice is prefigured at the juxtaposition of the ICM, the dPCM and the CM (Figure 1B, asterisk). This working model predicts that the dPCM is critical for the anorectum formation.

In this study, we test the cloaca occlusion hypothesis by functionally characterizing a signaling molecule Dickkopf-1 (*Dkk1*) during anorectal and genitourinary tract development. We demonstrate that *Dkk1* is highly expressed in the dPCMs but not the CM epithelial cells. Functionally, *Dkk1* mutants exhibit malformations including an imperforate anus with rectourinary fistula, a preputial hypospadias and a premature canalization of the genital urethra. *Dkk1* deletion results in a concerted upregulation of *Wnt, Shh, Fgf8* and *Bmp4* signals in the genital tubercle. Furthermore, genetic hyperactivation of the *Wnt/ß-catenin* signaling pathway partially recapitulates *Dkk1* mutant phenotypes. Together, these findings highlight the importance of the dPCM progenitors and establish *Dkk1* mutant allele as a valuable animal model to investigate etiology of the ARM. These findings further

suggest that development of the anogenital structures depends on a dynamic *Dkk1*-mediated inhibition of the canonical *Wnt/ß-catenin* signal pathway.

MATERIALS AND METHODS

Mice

All animal studies were performed according to protocols reviewed and approved by the institutional animal care and use committee at Boston Children's Hospital. Mouse lines, including *Dkk1* (MacDonald et al., 2004; Mukhopadhyay et al., 2001), $Six1^{Cre}$ (Wang et al., 2011), the *ß-catenin* GoF allele (Harada et al., 1999; Sun et al., 2012), Shh^{Cre} (Harfe et al., 2004) and $R26R^{mTmG}$ (Muzumdar et al., 2007) have previously been reported. Genotyping of the mice was performed as described.

Histology, Immunohistochemistry and in situ hybridization

We have described these procedures previously (Wang et al., 2011; Wang et al., 2013). In brief, staged embryos were dissected in cold phosphate buffer and fixed in 4% paraformaldehyde for subsequent analyses. Serial cryostat sections were used for histological analyses. Immunohistological staining was performed using cryostat sections. Whole-mount and section *in situ* hybridization were performed as described previously (Guo et al., 2011; Wang et al., 2011). Images were acquired with an Axioplan2 fluorescence microscope (Zeiss) or an Olympus SZX16 fluorescence dissection microscope equipped with a DP71 digital camera.

Cell proliferation and cell death analyses

Mitotic cells were labeled with the phospho-histone H3 Ser10 antibody (Upstate) and counter stained with a DNA-binding DAPI fluorescent dye (Molecular probe). Whole mount LysoTracker Red® (Invitrogen) vital dye labeling was performed according to the manufacturer's protocol. Stained embryos were fixed with paraformaldehyde and sectioned before image acquisition.

Real-time quantitative PCR

Microdissected genital tubercle tissue of e13.5 embryo was used for quantitative analyze gene expression level. RNA was extracted according to manufacturer's protocol (Qiagen RNAeasy mini). Relative gene expression levels were measured using SYBR Green Master Mix (Affymetrix) on an ABI-7500 detector (Applied BioSystems) and normalized to an internal control (18S RNA). The following oligos were used: 18S F: GTA ACC CGT TGA ACC CCA TT; 18S R: CCA TCC AAT CGG TAG TAG CG; Bmp4 F: GCC GAG CCA ACA CTG TGA GGA; Bmp4 R: GAT GCT GCT GAG GTT GAA GAG G; Fgf8 F: GGG AAG CTA ATT GCC AAG AG; Fgf8 R: TGT ACC AGC CCT CGT ACT TG; Shh F: ACG TAG CCG AGA AGA CCC TA; Shh R: ACT TGT CTT TGC ACC TCT GAG T; Axin2 F: GAC CGA CGA TTC CAT GTC CA; Axin2 R: CGG TGG GTT CTC GGA AAA TG.

RESULTS

Dkk1 is highly expressed in the dPCM progenitors

The cloaca occlusion model suggests that the dPCM is involved in establishing asymmetric growth of the cloacal mantle and formation of the anorectal structure (Figure 1) (Wang et al., 2011; Wang et al., 2013). To identify candidate genes that are important for normal anorectal development, we focused on secreted factors that are strongly expressed in the dPCM progenitors. To this end, we performed a detailed gene expression screening of

candidate signaling molecules and identified *Dkk1* (Figure 2), a known inhibitor of the canonical *Wnt/ß-catenin* pathway (Glinka et al., 1998; Mukhopadhyay et al., 2001).

The hindgut/cloacal cavity was visible from the ventral side of embryos at e10.0 prior to the genital tubercle formation (Figure 2A). *Dkk1* transcripts were detected bilaterally to the cloaca (Figure 2A). These two discrete domains correspond to sites where the Wolffian ducts insert into the cloaca (Kluth et al., 1995). *Dkk1* was continuously expressed near these sites at e10.5 but was undetectable at e11.0 when genital tubercle swellings were apparent (Figure 2C). At this stage, it was detected in the dPCM and vPCM progenitors but not the intermediate PCM (iPCM) located bilaterally to the CM (Figure 2B and C). These expression domains were confirmed by histological analysis of sections from whole mount stained embryos (Figure 2G-I). *Dkk1* expression in the dPCM was the highest at e11.5 (Figure 2D and H), when the juxtaposition of the ICM, dPCM and dorsal CM is observed (Figure 1B and 2H, asterisk). One day later, *Dkk1* expression in the dPCM diminished significantly and became undetectable in the vPCM (Figure 2E). *Dkk1* was also expressed in the genital tubercle, particularly at the dorsal and distal region beginning at e11.5 and persisted at e12.3 and e13.5 (Figure 2D-L). It was detected at both ectoderm epithelium and mesenchymal cells immediately underling the surface ectoderm of the developing genital tubercle (Figure 2H and I). However, we did not observe any *Dkk1* signal in the cloacal and urethral endodermal epithelial cells (Figure 2G-L).

Dkk1 mutants have an imperforated anus phenotype

To investigate potential roles of *Dkk1* during anorectal development, we analyzed the gross morphology of *Dkk1* null embryos (MacDonald et al., 2004; Mukhopadhyay et al., 2001). The digestive tract is an independent entity separated from the urinary tract at e15.5. This was apparent from a whole mount view of the micro-dissected lower urinary tract as the digestive tract was not physically connected to the urinary tract any longer (Figure 3A). In contrast to wild type littermate controls, the developing rectum was physically connected and communicating directly to the urethra in *Dkk1* mutants (Figure 3B). At late gestation stage (e17.5), no external opening of the digestive tract was observed from any of *Dkk1* mutants, indicating an imperforate anus phenotype (Figures 3C and D, n=5).

To further examine whether the rectum ended bluntly or ectopically connected to the urethra, we performed a systematic analysis of serial sagittal sections of staged embryos (Figures 3E-J). There was a clear separation between the anorectal and urogenital tracts at e12.5. The leading edge of the ICM had reached to the CM and dPCM, establishing a juxtaposition of these three tissues in wild type embryos (Figure 3E, inset, asterisk). Such juxtaposition failed to form in *Dkk1* mutants (Figure 3F). Instead, there was an ectopic dPCM tissue formation in the mutant, which significantly shortened the CM and displaced it from the juxtaposition. The overall size of the ICM and vPCM were comparable between controls and *Dkk1* mutants at this stage, which suggested that the putative urorectal septum was not affected (Figure 3E and 3F). At e14.5 and e16.5 when the anal canal was formed and completely separated from the urinary tract in controls, the anal canal was absent from *Dkk1* mutants (Figure 3G-J). The digestive tract of the mutants was connected ectopically to the urinary tract via a rectourinary fistula (Figures 3B, 3H and J, arrow). The fistula was located distally to the bladder neck region.

The midline epithelium of perineum has a unique embryonic origin that is derived from the *Shh*-positive cloacal endoderm including the CM (Seifert et al., 2008). Ectopic dPCM tissue formation correlated to a significant shortening of the CM in *Dkk1* mutants (Figure 3F). To ascertain this observation, we crossed *Dkk1* mutants into the compound heterozygous $Shh^{GC/+};R26R^{mTmG/+}$ genetic background (Harfe et al., 2004; Muzumdar et al., 2007). All *Shh*-positive genetic lineages including the cloaca endoderm-derived midline epithelium and

anal epithelium, as well as the preputial gland were labeled with *eGFP* signal (Figure 4A). The eGFP-positive lineages that corresponded to the prospective perineum and anal epithelium were not observed from *Dkk1* mutants. Consequently, overall length of the eGFP-labeled ventral midline epithelium were significantly shorter in *Dkk1* mutants (Figure 4, bracket), which provided additional support that the CM was shorter in *Dkk1* mutants (Figure 3F).

Taken together, deletion of *Dkk1* results in a ectopic tissue formation of the dPCM and shortening of the CM during early cloaca morphogenesis. Subsequently, these mutants develop the imperforate anus phenotype with a rectourinary fistula.

Dkk1 regulates PCM cell proliferation and survival

Ectopic tissue formation of *Dkk1* mutants suggested that *Dkk1* functionally restricted expansion of the dPCM tissue. To examine this possibility, we compared cell death and proliferation status (Figure 5). We stained serial sagittal sections using a mitotic marker, anti-phospho-histone H3 (p-HH3), to highlight proliferating cells (Guo et al., 2011; Wang et al., 2011). As early as e11.0, midline sagittal sections revealed an ectopic tissue formation at the dPCM region (Figures 5B and K). p-HH3-positive cells were detected in both the cloacal endoderm and the dPCM tissue (Figure 5A-C). In *Dkk1* mutants, a significant increase of total p-HH3-positive cells was observed in the dPCM tissue (Figure 5C). On the other hand, much fewer cells were found in the endoderm epithelium. An increase of dPCM cell proliferation was further confirmed when sagittal sections of e12.5 embryos were analyzed (Figures 5D and E). Furthermore, whole mount staining of e12.5 genital tubercles also showed an increase of p-HH3-positive cells at the ventral side of the genital tubercle (Figure 5F and G).

We next examined cell death by staining whole mount embryos using a vital dye LysoTracker Red® (Guo et al., 2011; Wang et al., 2011). As reported previously (Wang et al., 2011; Wang et al., 2013), wild type embryos had high levels of cell death near the tail gut and the distal urethral plate (Figure 5H-K). Gross examination revealed that mutant embryos had an overall reduction of LysoTracker Red® staining (Figures 5H and I). This finding was confirmed and became apparent when these stained embryos were re-examined by serial sagittal cryostat sections (Figures 5J and K). Together, these findings suggest that *Dkk1* controls normal behavior including proliferation and survival of the dPCM cells.

Premature urethra canalization of *Dkk1* mutants

Mutant genital tubercle was shorter along the proximodistal axis and wider along the mediolateral axis (Figures 3C and D). The distal urethral plate was flat and the urethral meatus was displaced to the base of genital tubercle (Figures 3C and D, insets), a phenotype reminiscent to the preputial hypospadias (Weiss et al., 2012). The genital tubercle defect was further examined at e15.5 (Figure 6), when it is morphologically identical between male and female (Suzuki et al., 2002). At this stage, the urethral fold but not the urethral tube was formed at the ventral side of the genital tubercle along the proximodistal axis (Figures 6A-D). Surprisingly, the urethral tube was already established in *Dkk1* null mutants (Figures 6E-H). The urethral epithelial structures were further confirmed by pan-cytokeratin immunoreactivity (Figures 6B, D, F and H). Therefore, *Dkk1* mutants have a premature urethral canalization but an incomplete urethral formation at late developmental stages (Figure 3D), resulting in a preputial hypospadias phenotype.

Activity of the *Wnt/ß-catenin* pathway is upregulated in *Dkk1* mutants

Dkk1 is a potent inhibitor of the canonical *Wnt/ß-catenin* signal pathway (Glinka et al., 1998; Mukhopadhyay et al., 2001). To begin to understand the underlying mechanism of the

imperforate anus phenotype of *Dkk1* mutants, we examined whether activity of the *Wnt/ß-catenin* signal was aberrantly enhanced in the mutant. Expression of *Axin2*, a downstream target gene, was used as a surrogate of the *Wnt/ß-catenin* activity (Jho et al., 2002; Lustig et al., 2002). The genital fold and the CM expressed low levels of *Axin2* in normal embryos at e11.0 (Figure 7A). The overall expression level in the genital fold was increased in *Dkk1* mutants (Figure 7B, arrow). Interestingly, *Axin2* expression in the dorsal but less so in the ventral of the CM was considerably higher in *Dkk1* mutants than wild type littermate controls (Figure 7B, arrowhead). We also observed an increase of *Axin2* signal in the hindlimb bud at the posterior edge (Figures 7B and D), consistent with the polydactyly phenotype of *Dkk1* mutants (MacDonald et al., 2004). Thus, *Dkk1* mutant embryos have abnormally high levels of the *Wnt/ß-catenin* activity.

Aberration of *Shh, Fgf8* and *Bmp4* gene expression in *Dkk1* mutants

Crosstalk between *Wnt* and *Shh* signal pathways are essential for growth and patterning of the genital tubercle (Lin et al., 2009; Miyagawa et al., 2009a). Endodermal *Shh* promotes cell cycle progression and enhances proliferation of mesenchymal cells and growth of the genital tubercle (Seifert et al., 2009; Seifert et al., 2010). Paracrine *Shh* signaling was shown to enhance *Wnt/ß-catenin* signaling, and hyperactivation of *ß-catenin* in the endoderm epithelium partially rescues the *Shh* mutant phenotype (Lin et al., 2009; Miyagawa et al., 2009a). Since *Dkk1* mutants had elevated *Wnt/ß-catenin* signaling, we next examined expression of other key signaling molecules (Figure 8).

Shh was detected at the endoderm epithelium of the genital tubercle at e12.5, as well as the preputial gland at e14.0 (Figures 8A and C). *Shh* was slightly reduced in *Dkk1* mutants at e12.5 (Figure 8B). Its' expression level, however, appeared to be increased at the proximal region of the urethral fold at a later stage (Figure 8D, bracket). More obviously, instead of the normal two spots of *Shh* expression at this stage, four spots of *Shh*-positive preputial glands were detected in *Dkk1* mutants. *Fgf8* is a downstream target of *Shh* and *Wnt* signaling pathways (Miyagawa 2009, Lin 2009, lin 2008, Seiffert 2009). *Fgf8* expression in the distal urethral plate was expanded in the mutant genital tubercle at e13.5, providing additional support that *Shh* and *Wnt* signaling were aberrantly upregulated in *Dkk1* mutants at these stages.

Expression of Bone morphogenetic protein 4 (*Bmp4*) in the genital tubercle mesenchymal cells also depends on the endodermal *Wnt* and *Shh* signals (Haraguchi et al., 2001; Lin et al., 2008; Lin et al., 2009; Perriton et al., 2002). *Bmp* signals promote cell death and attenuate growth of the genital tubercle (Suzuki et al., 2003). During limb development, *Dkk1* expression overlaps with the sites of apoptosis (Grotewold and Ruther, 2002). Furthermore, *Bmp4* upregulates *Dkk1* only when it concomitantly induces apoptosis, suggesting Bmp4 and Dkk1 synergistically regulate cell survival (Grotewold and Ruther, 2002; Mukhopadhyay et al., 2001). Mesenchymal cells surrounding the urethral fold expressed high levels of *Bmp4* at e12.5 (Figure 8G-J). Higher levels of *Bmp4* were detected in *Dkk1* mutants at the same developmental stage. One day later at e13.5, *Bmp4* expression was maintained, albeit weaker, in mesenchymal cells of wild type genital tubercle (Figure 8K). *Dkk1* mutants exhibited much stronger and broader *Bmp4* expression pattern (Figure 8L). Taken together, these results indicate that loss of *Dkk1* results in a concerted upregulation of *Wnt, Shh* and *Bmp4* signals during genitourinary tract development.

Cloaca morphogenesis depends on a dynamic inhibition of *Wnt/ß-catenin* signal

Dynamic *Dkk1* expression pattern suggested a potential significance of the spatiotemporal regulation of *Wnt/ß-catenin* signal during cloaca morphogenesis (Figure 2). We therefore examined to what extent that a constitutive activation of *ß-catenin* could mimic *Dkk1* mutant

phenotype (Figures 9 and 10). A conditional gain-of-function (GoF) *ß-catenin* allele was used to genetically activate *Wnt/ß-catenin* signal (Harada et al., 1999). We have used this mutant allele to modulate *Wnt/ß-catenin* signal during craniofacial development (Olson et al., 2006; Sun et al., 2012), and a similar strategy was used to interrogate functions of the *Wnt/ß-catenin* pathway during genital tubercle growth and patterning (Lin et al., 2008; Miyagawa et al., 2009a).

To conditionally activate *ß-catenin* in mesenchymal but not epithelial cells, we utilized a $Six1^{Cre}$ driver (Wang et al., 2011). Conditional *ß-catenin* GoF mutants survived to birth but died immediately after birth with severe craniofacial defects (data not shown). We chosen to focus on cell survival at early stage as significant cell death were detected in wild type embryos (Figures 5H and J). Whole mount LysoTracker staining revealed localized elevation of cell death in mesenchymal tissue bilateral to the CM and at the tail gut region in wild type embryos (Figure 9A-C). *ß-catenin* GoF mutants had diminished signal at the mesenchymal tissue, indicating a reduction of cell death (Figure 9D-F). Furthermore, expression of key signaling molecules, including *Bmp4*, *Fgf8* and *Shh*, as well as *Axin2* were significantly increased in the GoF mutant genital tubercles (Figure 9G), reminiscent to *Dkk1* mutants (Figure 8).

Similar to *Dkk1* mutants, genital tubercles of compound mutants were broader and less elongated than wild type littermate controls (Figure 10). The preputial fold failed to wrap around glans at the ventral side of the genital tubercle. The urethral meatus was closely located at the proximal region of the genital tubercle (Figure 10F, arrow). This preputial hypospadias phenotype resembled *Dkk1* mutant defects (compare Figure 3D and 10F). However, unlike imperforate anus defect found in *Dkk1* mutants, a small anal opening was observed in *ß-catenin* GoF mutants, indicating an anal stenosis phenotype (Figure 10F). To better visualize the anorectal canal, we injected Indian Ink from the large intestine to highlight lumens of the rectum and anal canal (Figures 10B and G). Consistent with gross observations, the anal canal of *ß-catenin* GoF mutants was narrower than wild type littermate controls (Figure 10G, n=5). To further characterize this phenotype, we analyzed serial histological cross sections of the anorectal structure. The normal anal canal is a smooth epithelial tube surrounded by condensing mesenchyme at e17.5 (Figure 10E), while the anal canal from the conditionally activated *ß-catenin* mutants was much narrower with increased amount of condensing mesenchyme (Figure 10J).

Taken together, these findings suggest that *Dkk1*-dependent dynamic control of the *Wnt/ß-catenin* signal is required for normal cloaca morphogenesis as a constitutive activation of the *Wnt/ß-catenin* signal in the cloacal mesenchyme only partially recapitulated *Dkk1* mutant phenotype.

DISCUSSION

Animal models are key to understanding the etiology of congenital human disorders but few have been employed to study ARMs (Kluth, 2010). One of the early reported ARM models was a herd of pigs with a hereditary imperforate anus defect (van der Putte, 1986), the Danforth's short tail (*Sd*) mouse mutant (Kluth et al., 1995; Nakata et al., 2009; Suda et al., 2011) and all-*trans* retinoic acid (ATRA)-treatment (Liu et al., 2003; Nakata et al., 2009). Results from studying these ARM models have led to the major revision of the classic cloaca septation model (Kluth et al., 1995; van der Putte, 1986). Here, we report that mouse *Dkk1* mutants have anorectal and genitourinary tract phenotypes. Our analyses of *Dkk1* mutant ARM model suggest that behavior of dPCM cells is critical for anogenital formation. These findings offer a critical support to the cloaca occlusion model (Wang et al., 2011; Wang et al., 2013), in which the dPCM cells and the CM are central in separating the cloaca

into the anorectal and genitourinary tracts (Figure 1). Results from this study further suggest that *Dkk1* is a candidate signal to regulate behavior of dPCM cells during normal cloaca morphogenesis.

Dkk1 mutant embryos have ectopic dPCM tissue and shortening of the CM (Figure 3). Since these anomalies are observed as early e11.0 prior to the septation of cloaca, these defects are likely the primary or early causes of imperforate anus phenotype. Indeed, the primordial anus structure, the juxtaposition of the ICM, CM and dPCM, is not observed in *Dkk1* mutant (Figure 3F). Origin of the ectopic tissue is unknown. Our findings suggest that it could be the result of increased proliferation and survival of the dPCM cell. However, these studies could not rule out a possibility of aberrant influx of migrating cells.

Dkk1 is a potent inhibitor of the *Wnt/ß-catenin* signal pathway (Glinka et al., 1998; Mukhopadhyay et al., 2001). Consistently, deletion of *Dkk1* leads to an elevation of the *Wnt/ß-catenin* activity as indicated by an increased expression of its downstream target gene *Axin2* in the hindgut region (Figure 7). *ß-catenin* GoF mutants partially recapitulate *Dkk1* mutant phenotype, including increased expression of key signaling molecules (Figure 9G), decreased cell death (Figure 9A-F), and preputial hyposapdias phenotype (Figure 10). Unexpectedly, *ß-catenin* GoF mutants have the anal stenosis instead of the imperforate anus phenotype. Since constitutive activation of *Wnt/ß-catenin* signal could not fully recapitulate timing, location and level of endogenous *Dkk1* activity, we suspect that normal cloaca morphogenesis most likely depends on the spatiotemporal inhibition of *Wnt/ß-catenin* signal pathway via *Dkk1*.

Dkk1 mutants exhibit premature canalization of the genital urethra (Figure 6). To our knowledge, this is the first report of mouse model with this condition. Genital urethra defect, such as hypospadias, is one of most common forms of birth defects (Blaschko et al., 2012; Weiss et al., 2012). The process of establishing sexual dimorphic external genitalia including formation of urethra depends on hormonal activities (Blaschko et al., 2012; Weiss et al., 2012; Yang et al., 2010). Interestingly, the *Wnt/ß-catenin* signal pathway exhibits a sexually dimorphic activity in which male genital tubercles have a stronger activity than female genital tubercle (Miyagawa et al., 2009b). Testosterone propionate treatment increases the *Wnt/ß-catenin* activity in the female genital tubercle (Miyagawa et al., 2009b). During early androgen-independent growth and patterning of the genital tubercle, *ß-catenin* is required for maintaining the homeostasis of urethral and ectoderm epithelia, and growth and patterning of the genital tubercle (Lin et al., 2008). Our findings suggest that *Dkk1* prevents premature canalization of genital urethra. It remains to be determined how *Dkk1* regulates urethra formation.

Acknowledgments

We would like to thank Ian Teng for his technical assistance. We particularly appreciate initial inputs from Gen Yamada and Peter V. Hauschka. This work was supported by grants from NIH/NIDCR (1R01DE019823, XL) and NIH/NIDDK (1R01DK091645-01A1, XL). BTM was supported by Xi He's grants (R01-GM057603 and R01-AR060359).

REFERENCES

Blaschko SD, Cunha GR, Baskin LS. Molecular mechanisms of external genitalia development. Differentiation. 2012

Cuschieri A. Anorectal anomalies associated with or as part of other anomalies. Am J Med Genet. 2002; 110:122–130.

Glinka A, Wu W, Delius H, Monaghan AP, Blumenstock C, Niehrs C. Dickkopf-1 is a member of a new family of secreted proteins and functions in head induction. Nature. 1998; 391:357–362.

Grotewold L, Ruther U. The Wnt antagonist Dickkopf-1 is regulated by Bmp signaling and c-Jun and modulates programmed cell death. Embo J. 2002; 21:966–975.

Guo C, Sun Y, Zhou B, Adam RM, Li X, Pu WT, Morrow BE, Moon A, Li X. A Tbx1-Six1/Eya1-Fgf8 genetic pathway controls mammalian cardiovascular and craniofacial morphogenesis. J Clin Invest. 2011; 121:1585–1595.

Harada N, Tamai Y, Ishikawa T, Sauer B, Takaku K, Oshima M, Taketo MM. Intestinal polyposis in mice with a dominant stable mutation of the beta-catenin gene. Embo J. 1999; 18:5931–5942.

Haraguchi R, Mo R, Hui C, Motoyama J, Makino S, Shiroishi T, Gaffield W, Yamada G. Unique functions of Sonic hedgehog signaling during external genitalia development. Development. 2001; 128:4241–4250.

Harfe BD, Scherz PJ, Nissim S, Tian H, McMahon AP, Tabin CJ. Evidence for an expansion-based temporal Shh gradient in specifying vertebrate digit identities. Cell. 2004; 118:517–528.

Hynes PJ, Fraher JP. The development of the male genitourinary system. I. The origin of the urorectal septum and the formation of the perineum. Br J Plast Surg. 2004; 57:27–36. [PubMed: 14672675]

Jho EH, Zhang T, Domon C, Joo CK, Freund JN, Costantini F. Wnt/beta-catenin/Tcf signaling induces the transcription of Axin2, a negative regulator of the signaling pathway. Mol Cell Biol. 2002; 22:1172–1183.

Kluth D. Embryology of anorectal malformations. Semin Pediatr Surg. 2010; 19:201–208.

Kluth D, Hillen M, Lambrecht W. The principles of normal and abnormal hindgut development. J Pediatr Surg. 1995; 30:1143–1147.

Lin C, Yin Y, Long F, Ma L. Tissue-specific requirements of {beta}-catenin in external genitalia development. Development. 2008; 135:2815–2825.

Lin C, Yin Y, Veith GM, Fisher AV, Long F, Ma L. Temporal and spatial dissection of Shh signaling in genital tubercle development. Development. 2009; 136:3959–3967. [PubMed: 19906863]

Liu Y, Sugiyama F, Yagami K, Ohkawa H. Sharing of the same embryogenic pathway in anorectal malformations and anterior sacral myelomeningocele formation. Pediatr Surg Int. 2003; 19:152–156.

Lustig B, Jerchow B, Sachs M, Weiler S, Pietsch T, Karsten U, van de Wetering M, Clevers H, Schlag PM, Birchmeier W, Behrens J. Negative feedback loop of Wnt signaling through upregulation of conductin/axin2 in colorectal and liver tumors. Mol Cell Biol. 2002; 22:1184–1193.

MacDonald BT, Adamska M, Meisler MH. Hypomorphic expression of Dkk1 in the doubleridge mouse: dose dependence and compensatory interactions with Lrp6. Development. 2004; 131

Miyagawa S, Moon A, Haraguchi R, Inoue C, Harada M, Nakahara C, Suzuki K, Matsumaru D, Kaneko T, Matsuo I, Yang L, Taketo MM, Iguchi T, Evans SM, Yamada G. Dosage-dependent hedgehog signals integrated with Wnt/beta-catenin signaling regulate external genitalia formation as an appendicular program. Development. 2009a; 136:3969–3978.

Miyagawa S, Satoh Y, Haraguchi R, Suzuki K, Iguchi T, Taketo MM, Nakagata N, Matsumoto T, Takeyama K, Kato S, Yamada G. Genetic interactions of the androgen and Wnt/beta-catenin pathways for the masculinization of external genitalia. Mol Endocrinol. 2009b; 23:871–880.

Mukhopadhyay M, Shtrom S, Rodriguez-Esteban C, Chen L, Tsukui T, Gomer L, Dorward DW, Glinka A, Grinberg A, Huang SP, Niehrs C, Izpisua Belmonte JC, Westphal H. Dickkopf1 is required for embryonic head induction and limb morphogenesis in the mouse. Dev Cell. 2001; 1:423–434.

Muzumdar MD, Tasic B, Miyamichi K, Li L, Luo L. A global double-fluorescent Cre reporter mouse. Genesis. 2007; 45:593–605.

Nakata M, Takada Y, Hishiki T, Saito T, Terui K, Sato Y, Koseki H, Yoshida H. Induction of Wnt5a-expressing mesenchymal cells adjacent to the cloacal plate is an essential process for its proximodistal elongation and subsequent anorectal development. Pediatr Res. 2009; 66:149–154.

Olson LE, Tollkuhn J, Scafoglio C, Krones A, Zhang J, Ohgi KA, Wu W, Taketo MM, Kemler R, Grosschedl R, Rose D, Li X, Rosenfeld MG. Homeodomain-mediated beta-catenin-dependent switching events dictate cell-lineage determination. Cell. 2006; 125:593–605.

Paidas CN, Morreale RF, Holoski KM, Lund RE, Hutchins GM. Septation and differentiation of the embryonic human cloaca. J Pediatr Surg. 1999; 34:877–884.

Penington EC, Hutson JM. The absence of lateral fusion in cloacal partition. J Pediatr Surg. 2003; 38:1287–1295.

Perriton CL, Powles N, Chiang C, Maconochie MK, Cohn MJ. Sonic hedgehog signaling from the urethral epithelium controls external genital development. Dev Biol. 2002; 247:26–46.

Rathke, H. Abhandlungen zur Bildungs- und Entwicklungsgeschichte der Tiere. Leipzig: 1832.

Retterer E. Sur l'origine et l'evolution de la region anogenitale des mammiferes. Journal of Anatomy (Paris). 1890; 26:126–216.

Seifert AW, Bouldin CM, Choi KS, Harfe BD, Cohn MJ. Multiphasic and tissue-specific roles of sonic hedgehog in cloacal septation and external genitalia development. Development. 2009; 136:3949–3957.

Seifert AW, Harfe BD, Cohn MJ. Cell lineage analysis demonstrates an endodermal origin of the distal urethra and perineum. Dev Biol. 2008; 318:143–152.

Seifert AW, Zheng Z, Ormerod BK, Cohn MJ. Sonic hedgehog controls growth of external genitalia by regulating cell cycle kinetics. Nat Commun. 2010; 1:1–9.

Stephens, DF.; Smith, DE.; Hutson, JM. Congenital anomalies of the kidney, urinary and genital tracts. 2nd ed.. 2002.

Suda H, Lee KJ, Semba K, Kyushima F, Ando T, Araki M, Araki K, Inomata Y, Yamamura KI. The Skt gene, required for anorectal development, is a candidate for a molecular marker of the cloacal plate. Pediatr Surg Int. 2011

Sun Y, Teng I, Huo R, Rosenfeld MG, Olson LE, Li X, Li X. Asymmetric requirement of surface epithelial beta-catenin during the upper and lower jaw development. Dev Dyn. 2012; 241:663–674.

Suzuki K, Bachiller D, Chen YP, Kamikawa M, Ogi H, Haraguchi R, Ogino Y, Minami Y, Mishina Y, Ahn K, Crenshaw EB 3rd, Yamada G. Regulation of outgrowth and apoptosis for the terminal appendage: external genitalia development by concerted actions of BMP signaling [corrected]. Development. 2003; 130:6209–6220. [PubMed: 14602679]

Suzuki K, Ogino Y, Murakami R, Satoh Y, Bachiller D, Yamada G. Embryonic development of mouse external genitalia: insights into a unique mode of organogenesis. Evol Dev. 2002; 4:133–141.

Tourneux F. Sur les premiers developpements du cloaque du tubercle genitale et de l'anus chez l'embryon de mouton. Journal of Anatomy (Paris). 1888; 24:503–517.

van der Putte SC. Normal and abnormal development of the anorectum. J Pediatr Surg. 1986; 21:434–440.

Wang C, Gargollo P, Guo C, Tang T, Mingin G, Sun Y, Li X. Six1 and Eya1 are critical regulators of peri-cloacal mesenchymal progenitors during genitourinary tract development. Dev Biol. 2011; 360:186–194.

Wang C, Wang J, Borer JG, Li X. Embryonic origin and remodeling of the urinary and digestive outlets. PLoS One. 2013; 8:e55587.

Weiss DA, Rodriguez E Jr. Cunha T, Menshenina J, Barcellos D, Chan LY, Risbridger G, Baskin L, Cunha G. Morphology of the external genitalia of the adult male and female mice as an endpoint of sex differentiation. Mol Cell Endocrinol. 2012; 354:94–102.

Yang JH, Menshenina J, Cunha GR, Place N, Baskin LS. Morphology of mouse external genitalia: implications for a role of estrogen in sexual dimorphism of the mouse genital tubercle. J Urol. 2010; 184:1604–1609.

HIGHLIGHTS

1. *Dkk1* is highly expressed and required for behavior of the dPCM progenitors.
2. *Dkk1* mutants have an imperforate anus phenotype with rectourinary fistula.
3. Deletion of *Dkk1* causes premature urethra canalization.
4. Anogenital development depends on *Dkk1*-mediated dynamic inhibition of the *Wnt/ß-catenin* pathway.
5. *Dkk1* is highly expressed and required for behavior of the dPCM progenitors.
6. *Dkk1* mutants have an imperforate anus phenotype with rectourinary fistula.
7. Deletion of *Dkk1* causes premature urethra canalization.
8. Anogenital development depends on *Dkk1*-mediated dynamic inhibition of the *Wnt/ß*-catenin pathway.

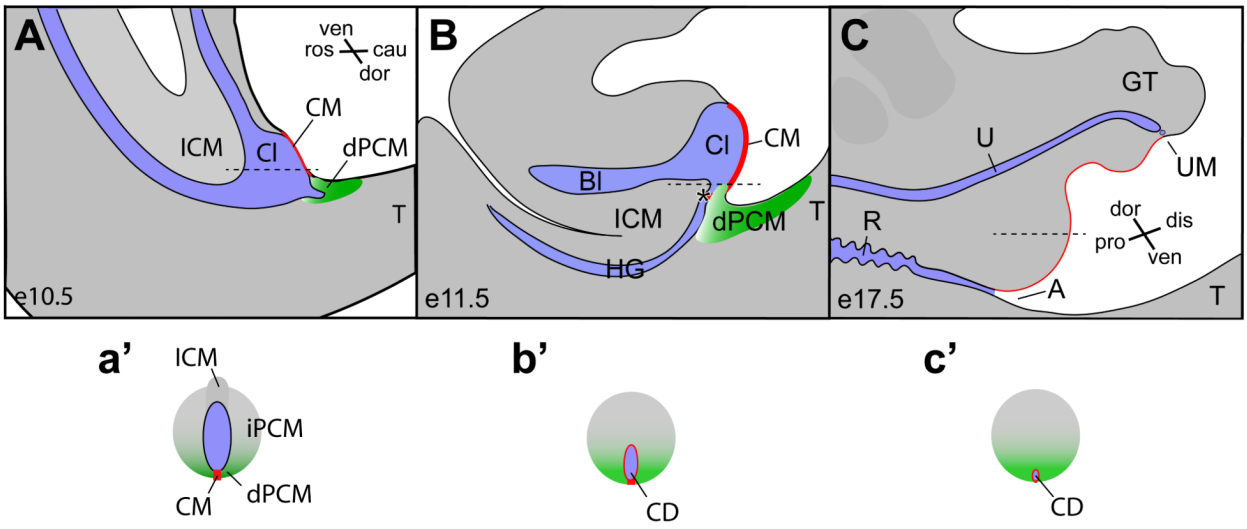

Figure 1. The occlusion model of cloaca morphogenesis

The cloaca occlusion model suggests that the dorsal peri-cloacal mesenchyme (dPCM, green) and the cloacal membrane (CM, red) play prominent roles in morphogenesis of the cloaca (Cl). blue, endoderm cavity. The CM and the dPCM function as two pivot points through which asymmetric growth of mesenchymal cells surrounding cloacal leads to separation of the hindgut (HG) and developing bladder (Bl), as well as outgrowth of genital tubercle (GT). Both midline sagittal views (**A-C**) and horizontal views (**a'**-c', indicated in A-C as dash lines) are shown. A, anus; Bl, bladder; Cl, cloaca; cau, caudal; dis, distal; dor, dorsal; ICM, intra-cloacal mesenchyme; pro, proximal; R, rectum; ros, rostra; T, tail; ven, ventral; asterisk, juxtaposition of the ICM, the dPCM and the CM.

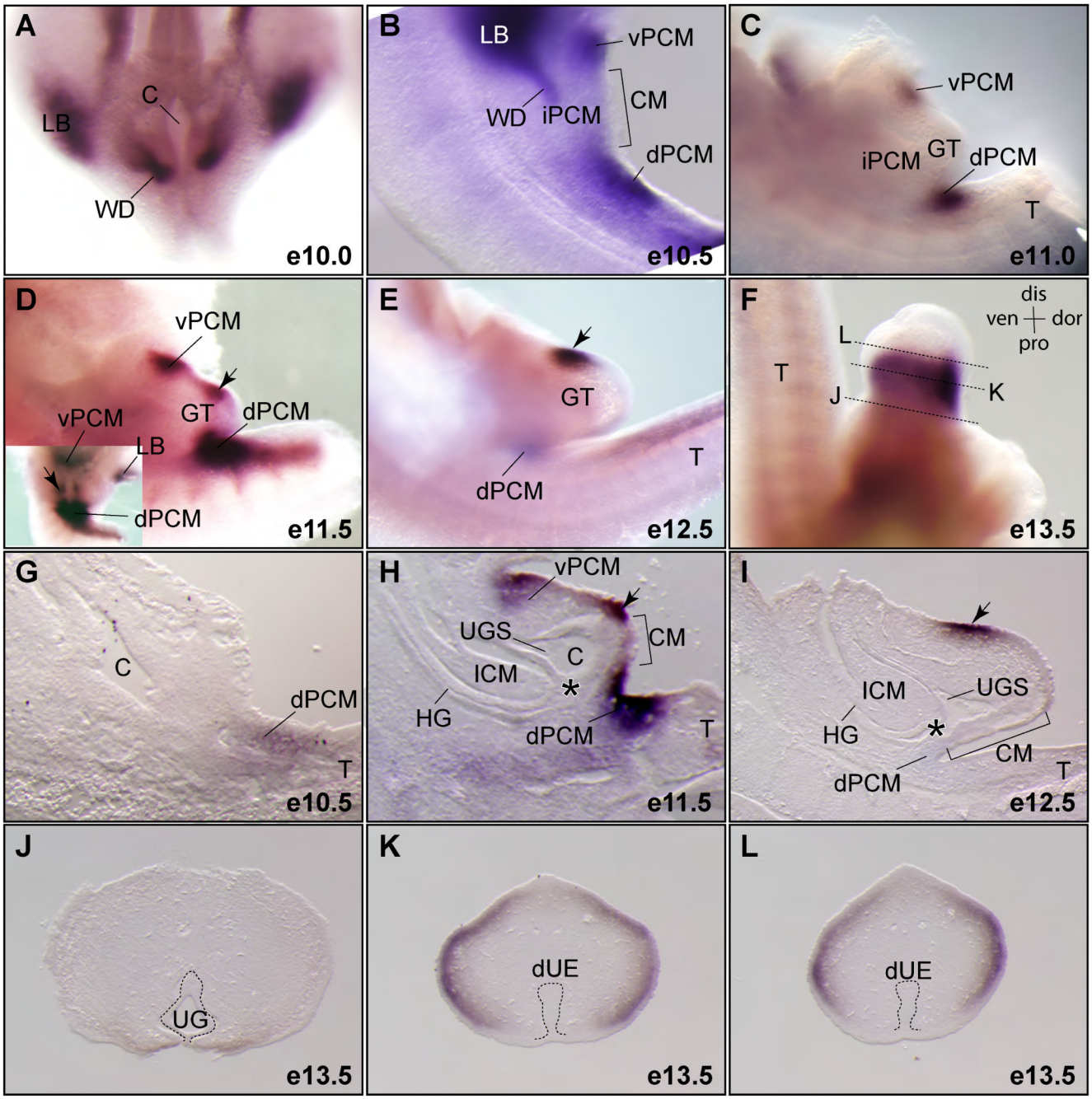

Figure 2. Dynamic expression pattern of *Dkk1* during cloaca morphogenesis

(**A-F**) Whole mount RNA *in situ* hybridization using a *Dkk1* specific probe (n=2). All images are lateral views except A and an inset in D, which are ventral views. (**G-I**) Midline sections of *Dkk1* whole mount stained embryos. (**J-L**) Cross sections of the genital tubercle of a e13.5 embryo shown in F. dUE, distal urethral epithelium; LB, limb bud; UG, urethral groove; vPCM, ventral peri-cloacal mesenchyme; WD, Wolffian ducts; asterisk, juxtaposition of the ICM, the dPCM and the CM. See Figure 1 for more abbreviations.

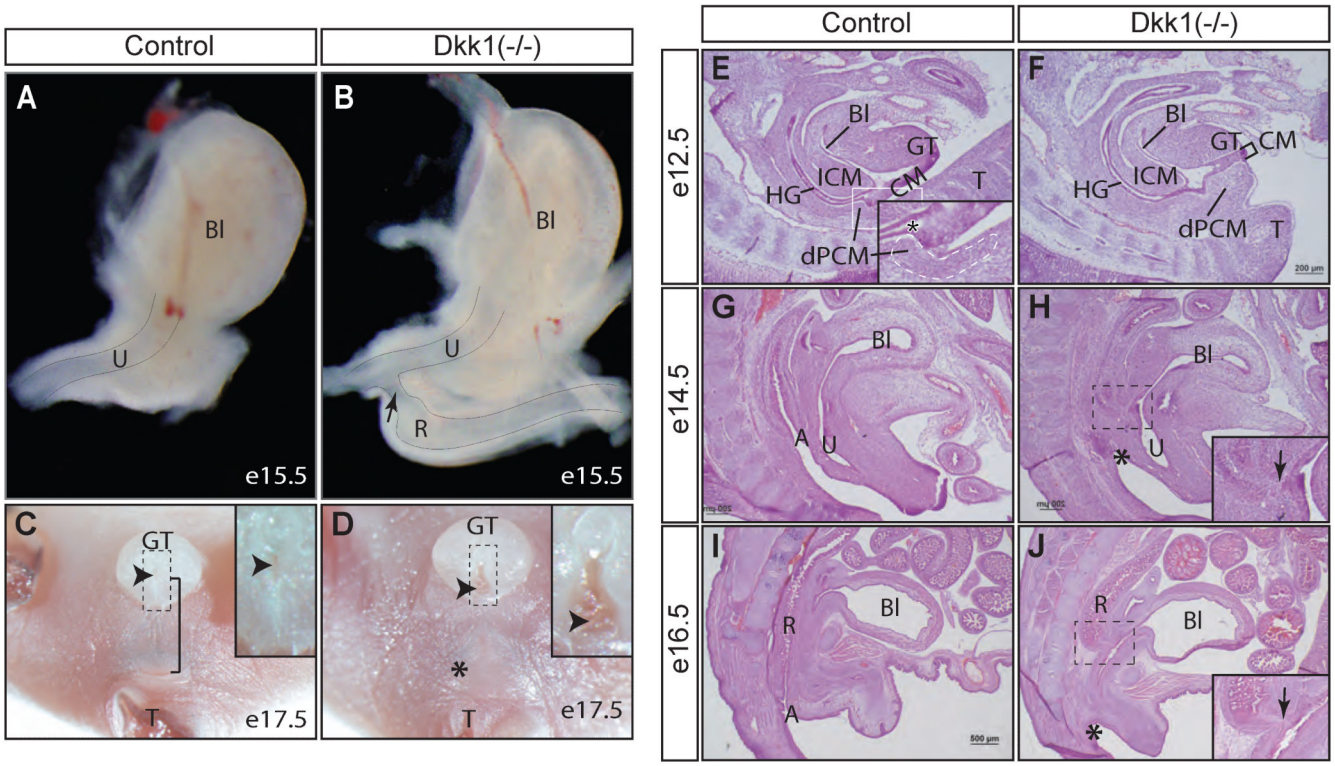

Figure 3. ***Dkk1*** **mutants exhibit an imperforate anus with rectourinary fistula**

(**A** - **D**), whole mount views of lower urinary tract at e15.5 (A and B, lateral view, n=3) and anogenital structures at e17.5 (C and D, ventral view, n=5). Insets in C and D show the urethral meatus (arrowhead). Bracket, anogenital distance; Asterisk, missing anus. (**E**- **J**) Histological midline sagittal sections from staged embryos (n=2 from each stage). Insets in H and J indicate the rectourinary fistula (arrow). See Figures 1 and 2 for more abbreviations.

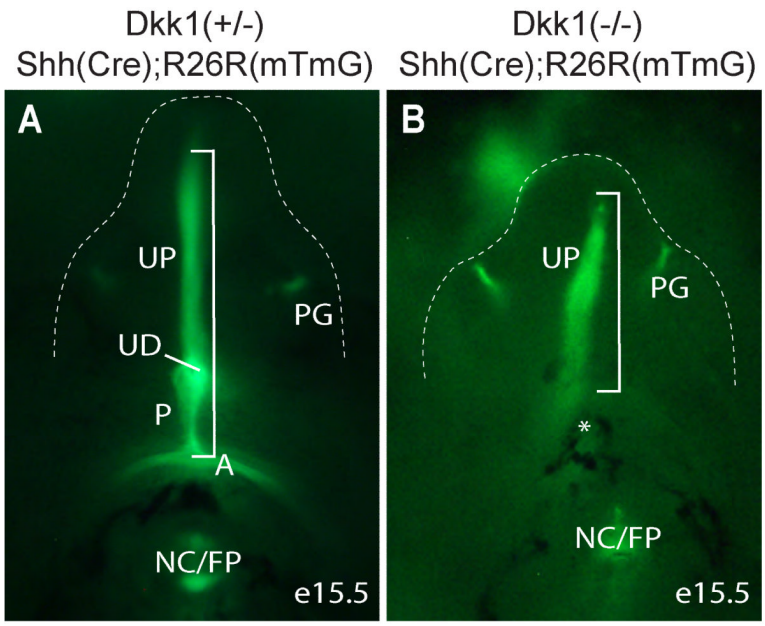

Figure 4. Genetic lineage mapping of *Shh*-expression cells

Ventral view *eGFP*-positive *Shh* lineages of e15.5 genital tubercle (outlined) and perineum. A, anus; NC/FP, notochord/floor plate; P, perineum; PG, preputial gland; UD, urethra duct; UF, urethral fold; asterisk, denote missing anus and perineum; bracket, ventral midline endoderm derived epithelium from anus to distal urethral plate.

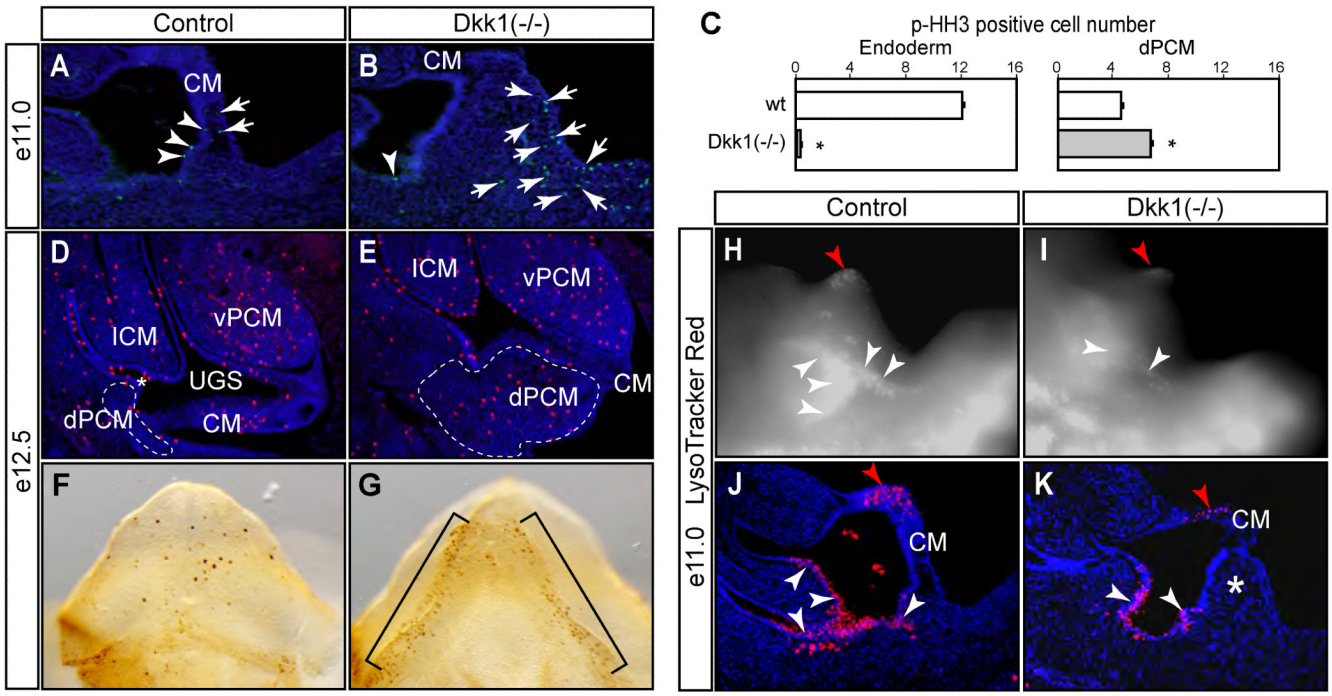

Figure 5. Proliferation and apoptosis defects of *Dkk1* mutants

(**A-E**) A mitotic marker phospho-histone H3 (p-HH3) staining of midline sagittal sections (A-E) and whole mount genital tubercle (F and G, ventral views). Results from e11.0 embryos are quantified in C. Total p-HH3-positive mesenchyme (arrow) and endoderm (arrowhead) cells from each section are counted separately. Asterisk, $p<0.05$, Student *t* test, n=3. (**H-K**) LysoTracker Red® staining of e11.0 wild type control (H and J) and *Dkk1* mutant (I and K). Positive signals appeared to be bright white in whole mount images (H and I) and red in midline sagittal sections (J and K). Double asterisk, ectopic dPCM tissue. Red arrowhead, distal urethral plate epithelium.

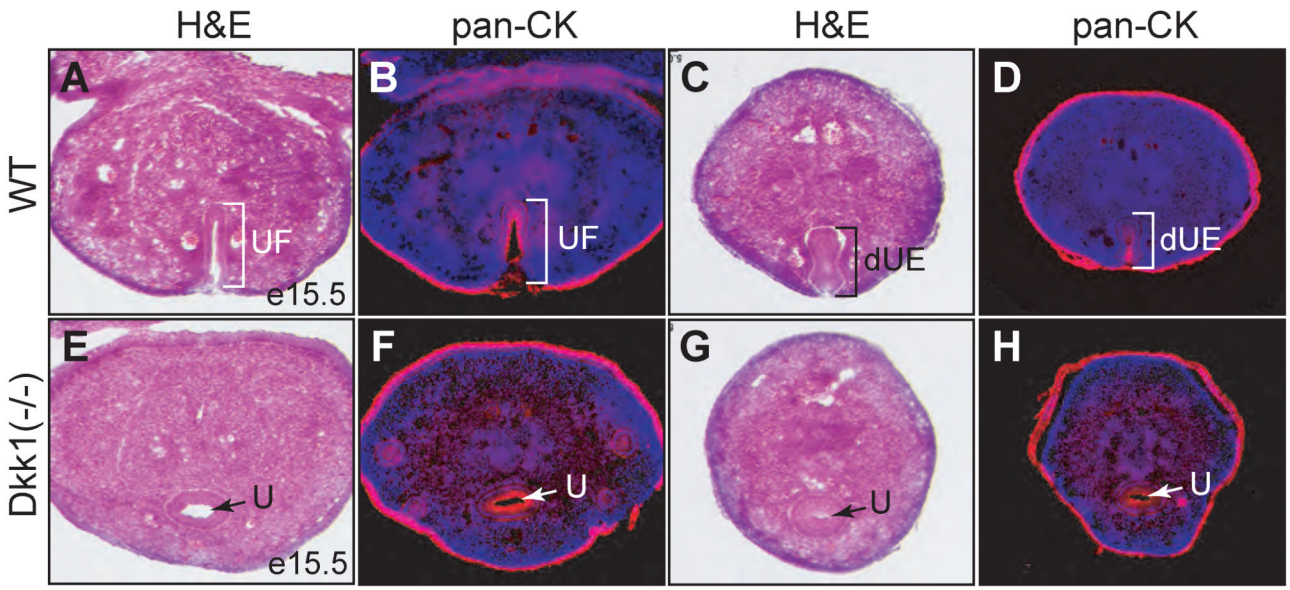

Figure 6. Deletion of *Dkk1* causes premature canalization of the genital urethra

Histological and pan-cytokeratin immunostaining of adjacent cross sections from e15.5 control (A-D) or *Dkk1* mutant (E-H) genital tubercles. dUE, distal urethral epithelia; U, urethra; UF, urethral fold.

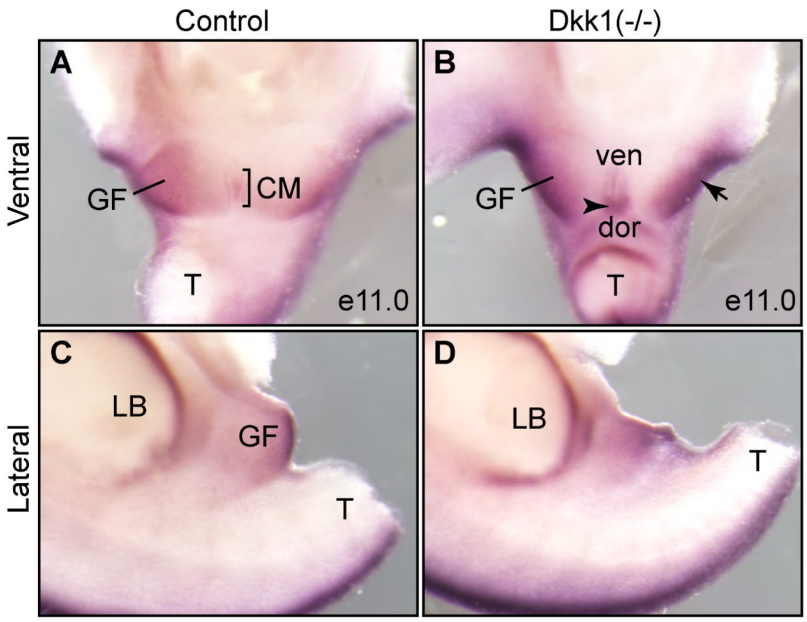

Figure 7. *Axin2*, an indicator of the *Wnt/ß-catenin* activity, is upregulated

Whole mount RNA *in situ* of e11.0 urogenital structures from control (A and C) and *Dkk1* mutant (B and D) using *Axin2* probe (n=3). Both ventral (A and B) and lateral (C and D) views were shown. CM, cloacal membrane; dor, dorsal; GF, genital fold; LB, limb bud; T, tail; ven, ventral; arrow, enhanced expression in the GF; arrowheaad, enhanced expression in the dorsal CM.

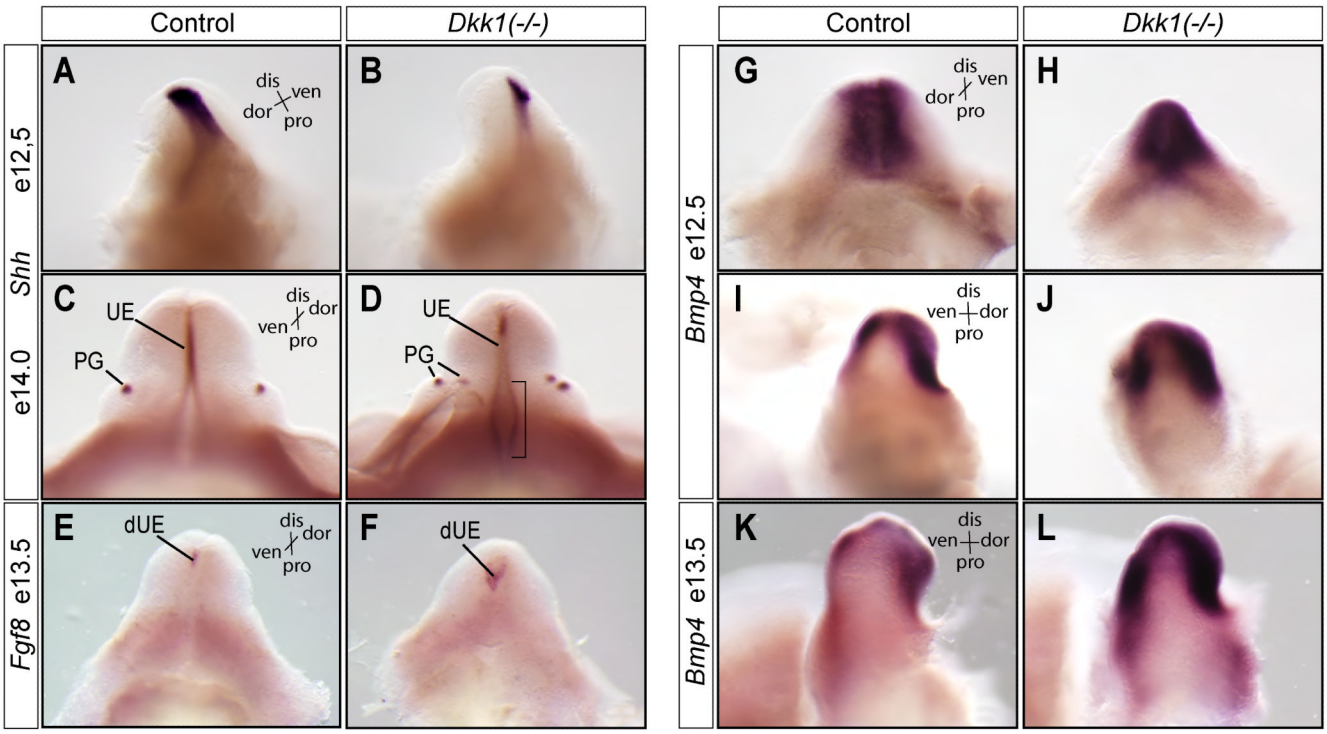

Figure 8. Aberrant expressions of *Shh, Fgf8* and *Bmp4* in the mutant genital tubercles

(**A-D**) Whole mount RNA *in situ* hybridizations using *Shh* (A-D), *Fgf8* (E and F) and *Bmp4* (G-L) probes (n=2). dis, distal; dor, dorsal; pro, proximal; ven, ventral; UE, erethral epithelia; PG, preputial gland; dUE, distal urethral epithelia; bracket, proximal urethral fold epithelia.

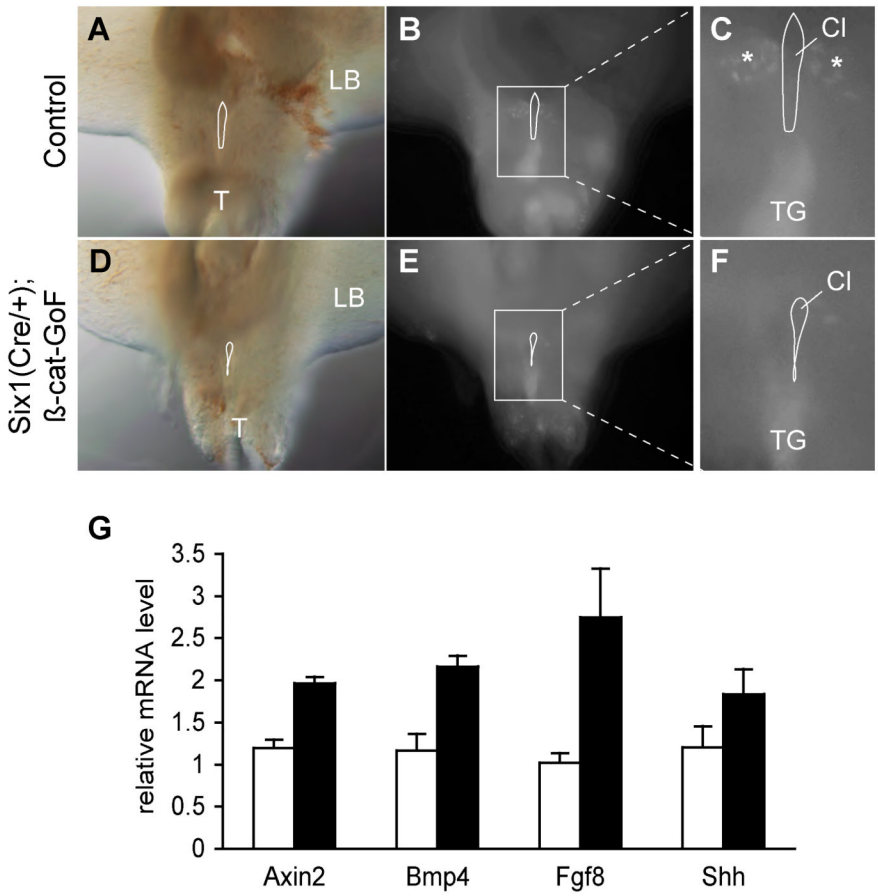

Figure 9. Constitutive activation of *ß-catenin* in the PCM

(**A**-**F**) Ventral views of LysoTracker stained e10.5 embryos from control (A-C) and *ß-catenin* GoF mutants (D-F). A and D, visual light images; B and E, fluorescent images of labeled cells; enlarged views are shown in C and F. Cl, cloaca; T, tail; TG, tail gut. (**G**) Significant increase of marker gene expression in *ß-catenin* GoF mutants (*Student*-t test, n=3). Real time quantitatively PCR analysis of expression of specific genes in e13.5 genital tubercle using 18S RNA as an internal control. Open column, littermate control; solid column, $Six1^{Cre/+}$;*ß-cateinn-GoF* mutants.

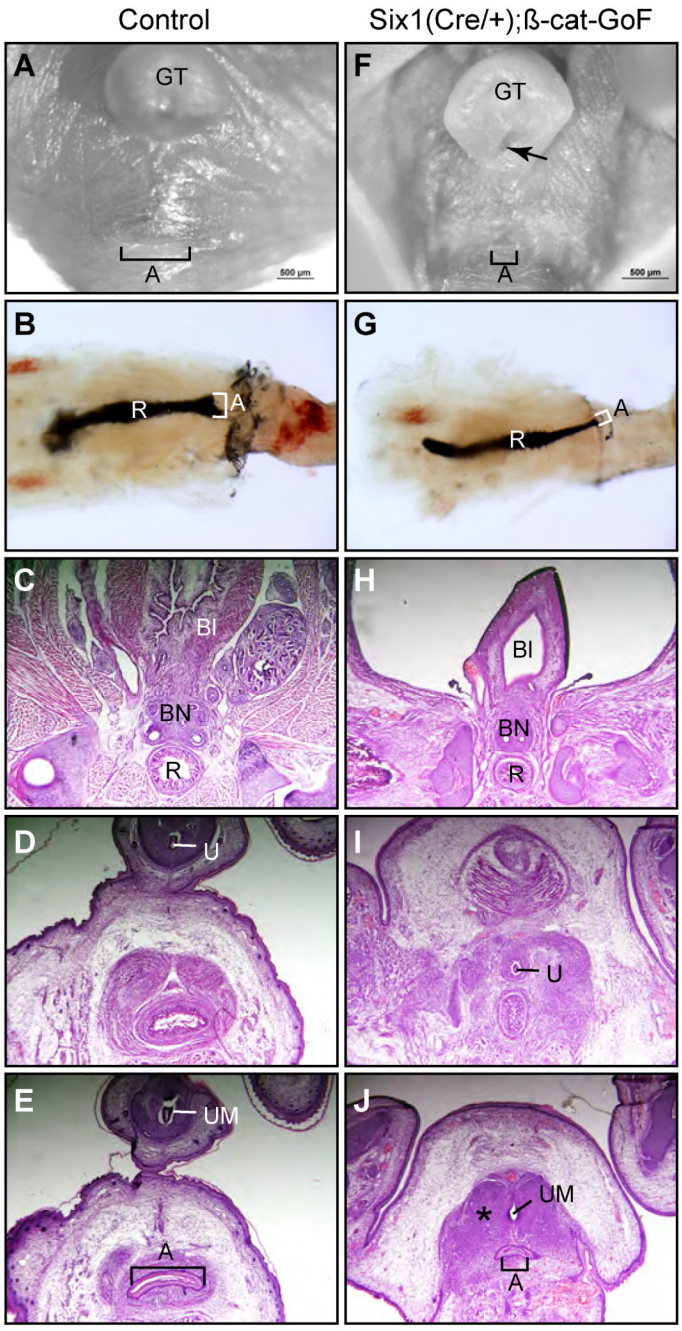

Figure 10. *ß-catenin* GoF mutants partially recapitulate the urogenital phenotypes of *Dkk1* mutants

(**A** and **F**) Whole mount ventral view of urogenital structures from e17.5 wild type control (A) and *Six1*$^{Cre/+}$*;ß-Cat-GoF* compound mutants (F). (**B** and **G**) India Ink paint injection of anorectal lumen (n=5). (**C**-**E** and **H**-**J**) Serial histology of cross sections of the anal canal from e17.5 male embryos. A, anus; Bl, bladder; BN, bladder neck; GT, genital tubercle; R, rectum; U, genital urethra; UM, urethra meatus; asterisk, ectopic mesenchymal condensation (n=3).